The Cytotoxicity, DNA Fragmentation, and Decreasing Velocity Induced by Chromium (III) Oxide on Rainbow Trout Spermatozoa

Mustafa Erkan Özgür (aquaclubkemaliye@yahoo.com)
Malatya Turgut Ozal University, Department of Aquaculture, Faculty of Fishery https://orcid.org/0000-0002-2966-9627

Ahmet Ulu
İnönü Üniversitesi: Inonu Universitesi

Canbolat Gürses
Inonu University: Inonu Universitesi

İmren Özcan
Inonu University: Inonu Universitesi

Samir Abbas Ali Noma
Inonu University: Inonu Universitesi

Süleyman Köytepe
Inonu University: Inonu Universitesi

Burhan Ateş
Inonu University: Inonu Universitesi

Research Article

Keywords: Cr2O3 , Cytotoxicity , Oncorhynchus mykiss , Spermatozoa , DNA damages

Posted Date: May 24th, 2021

DOI: https://doi.org/10.21203/rs.3.rs-497860/v1

Version of Record: A version of this preprint was published at Biological Trace Element Research on April 4th, 2022. See the published version at https://doi.org/10.1007/s12011-022-03211-9.

Abstract

The present study aimed to determine the cytotoxicity of Chromium (III) oxide micro particles (Cr_2O_3-Ps) in rainbow trout (*Oncorhynchus mykiss*) spermatozoa. Firstly, Cr_2O_3-Ps were synthesized and structurally characterized the surface, morphological for particle size and thermal properties. In addition, its structural and elemental purity was determined using EDX spectrum and elemental maps. Structural purity, thermal properties, and stability of Cr_2O_3-Ps were also examined in detail by performing thermal analysis techniques. The cytotoxicity of structurally defined Cr_2O_3-Ps was measured by the observation of velocities, antioxidant activities, and DNA damages in spermatozoa after exposure in vitro. The straight line velocity (VSL), the curvilinear velocity (VCL), and the angular path velocity (VAP) of spermatozoa decreased after exposure to Cr_2O_3-Ps. While the superoxide dismutase (SOD) and the catalase (CAT) decreased, the lipid peroxidation increased in a dose-dependent manner. However, the total glutathione (tGSH) did not affect in this period. DNA damages was also determined in spermatozoa using Comet assay. According to DNA in tail (%) data, DNA damages have been detected with gradually increasing concentrations of Cr_2O_3-Ps. Furthermore, all of class types related to DNA fragmentation has been observed between 50 µg/L and 500 µg/L concentrations of Cr_2O_3-Ps exposed to rainbow trout spermatozoa. At the end of this study, we determined that the effective concentrations (EC50) were 76.67 µg/L for VSL and 87.77 µg/L for VCL. Finally, these results about Cr_2O_3-Ps may say to be major risk concentrations over 70 µg/L for fish reproduction in aquatic environments.

Introduction

In recently, although the growth rate in using metal oxide particles have been increased due to their characteristics such as huge specific surface areas, micro interface characteristics, and remediation ability, they can have many potential environmental risks (Du et al. 2019; Zhu et al. 2019). Metal oxides have been the focus of attention in many studies with their superior electrical properties, thermal stability, and extraordinary morphology (Chavali and Nikolova 2019). They also have an increasing use in many industries such as semiconductors, catalysts, solar panels, and UV protectors. Cr_2O_3 has a very important place among metal oxides, which have a very wide variety. Besides being used in many electronic applications with approximately 3eV band spacing, it is used in industrial applications such as paint, pigment, catalyst, solar panels, wear resistant materials, thermal protection, electrochromic material, and hydrogen storage. This widespread use of Cr_2O_3 brings some environmental concerns.

Anthropogenic sources have many effects that can contaminate aquatic life and these have also toxic agents. However, many toxic contaminants pollute the water system. One of them, Chromium (Cr) is a major metallic element posing a maximum threat to all animals and plants according to US-Environmental Protection Agency (US-EPA). The main sources of chromium entering the aquatic environment can reach from dyes, mining, electroplating, automobile, and textile manufacturing, metal processing and leather tanning (Canadian Water Quality Guidelines 1999; EPA 2015; Maitlo et al. 2019). However, while it is estimated that the production amounts of manufactured metal oxide nano or micro

materials in 2020 are 1.663.168 tons (He et al. 2015), the production of Chromium in the world is 44.000 gross weight in 2019 (U.S Geological Survey 2020).

In the modern industry, Chromium (III) oxide particles (Cr_2O_3-Ps) also started to use in pigments for ceramics, dyes, paints, and cosmetics (Puerari et al. 2016). But unfortunately, there is no more information about the toxicological characteristics of this micro material on reproduction system of fish. The US Environmental Protection Agency (EPA) has set a maximum concentration level (MCL) of 100 µg/L for chromium discharged into waters, because it is very toxic (EPA 2015). Due to the data that even very small amounts of chromium can be toxic, it was become a hot topic to investigate the relationships with water environments for this study.

In a broader context, there are not more studies that addressed the toxicity of Cr_2O_3-Ps in the literature. In the light of the literature, if we give some examples, researchers studied on the lung cells (BEAS-2B) and bronchoalveolar carcinoma-derived cells (A549) of human (Cho et al. 2013; Chusuei et al. 2013), bacteria in in activated sludge system (Wang et al. 2017), green alga (Costa et al. 2015), freshwater micro crustacean *Daphnia magna* and marine bacterium *Aliivibrio fischeri* (Puerari et al. 2016), *Daphnia smilis* (Tavares et al. 2014), *Escherichia coli* (Kaweeteerawat et al. 2015), Wistar rats (Lebedev et al. 2018) and soybean (*Glycine max*) (Li et al. 2018). In light of these literatures, we couldn't also find any study about Cr_2O_3-Ps toxicity on fish or fish reproduction. For both no many studies and there are more productive and using of chromium, this study has been designed since it has become a need to conduct scientific research on Cr_2O_3-Ps. Thus, this study was carried out to determine the cytotoxicity of Cr_2O_3-Ps on reproduction of rainbow trout (*Oncorhynchus mykiss*) with *in vitro* assay. Because it is known that *in vitro* methods have helped to determine the toxicity levels of environmental pollutants, the mechanisms, exposure times, concentrations (Özgür et al. 2019). For this aim, target particles were exposed on the spermatozoa of rainbow trout and it was investigated the velocities, movement styles, oxidative stress indices, effective concentrations, and DNA damages of spermatozoa.

Materials And Methods

Chemicals

In this study, the decomposition reaction of ammonium dichromate at high temperatures was used in the synthesis of Cr_2O_3-Ps. Accordingly, all chemicals used during synthesis and purification were obtained from Sigma-Aldrich. These chemicals used were preferred in analytical purity and were used without any purification process.

Instrumentation

The chemical structures of the obtained Cr_2O_3-Ps were measured in the range of 400–4000 cm^{-1} using Perkin Elmer Spectrum Two model FTIR device. Crystal property and purity of Cr_2O_3-Ps were carried out using Rigaku Rad B-Dmax II powder brand X-ray device and were measured in the range of 20–80 2-theta.

Structural and morphological properties of Cr_2O_3-Ps were measured with the LEO EVO-40xVP model SEM device after coating with Au-Pd conductive coating using a Bal-tec brand spatter. Bruker brand Rönteck Xflash EDX detector connected to SEM device was used for elemental verification of Cr_2O_3-Ps structure. Particle size analyzes of the obtained Cr_2O_3 particles were carried out by using Malvern Zetasizer Nano-ZS model device by dispersing it in water. Shimadzu DTA-50 and Shimadzu TGA-50 devices were used to determine the thermal stability of the synthesized Cr_2O_3-Ps, and the analyses were carried out between 30-1000°C using 10°C/min heating rate in the air atmosphere and used about 10 mg sample in Pt sample pan.

Preparation and characterization of Cr_2O_3-Ps

Cr_2O_3-Ps were prepared by thermal decomposition of ammonium dichromate in accordance with the literature (Mahieu et al. 1971; Galwey et al. 1983). First, ammonium dichromate was mixed with ethanol. It was burned at a high temperature in a controlled manner. When the entire mixture turned green, the resulting Cr_2O_3 was washed with ethanol. It was dried in an oven at 110 ° C for 3 hours. It was ground and its chemical structure, morphology, and purity were checked.

Experimental design

Semen samples were collected from rainbow trout (*Oncorhynchus mykiss*, Walbaum, 1792) males (1900 ± 150 g) which were supplied from a commercial farm in Malatya, Turkey in January 2020. Semen samples were obtained by massage method from the front to the back of the male fish abdomen without anesthesia. The semen pool was taken from 7 individuals of fish. Fresh semen samples in semen pool were diluted with inhibition solution of spermatozoa motility or inactivation solution (IS) (NaCl, 103 mmol/L; KCl, 40 mmol/L; $CaCl_2$, 1 mmol/L; $MgSO_4$, 0.8 mmol/L; Hepes, 20 mmol/L (Özgür et al., 2018); pH 7.8, adjusted with 1 N-NaOH) as a stock solution. The pooled sample was diluted with IS at ratio 1:10 (Semen:IS) to obtain a spermatozoa density of about 12×10^8 cells/mL.

In vitro exposure of Cr_2O_3-Ps was carried out on a semen pool. The semen sub-samples were exposed with nominal concentrations such as 10, 50, 100, 500, and 1000 µ/L of Cr_2O_3-Ps at 4°C for 3 h in Eppendorf tubes with the lid closed. The exposure the concentrations of Cr_2O_3-Ps were determined according to maximum concentration level of Chromium that is 100 µ/L in EPA (EPA 2015). Semen sub-samples exposed with Cr_2O_3-Ps at the ratio of 1:20 (Cr_2O_3-Ps: Semen with IS) in Eppendorf tubes.

The velocities and movement style of spermatozoa

The velocities and movement style parameters of spermatozoa were analyzed by the computer assisted semen analysis system (CASA). The values of velocity parameters such as VSL (straight line velocity, µm/s), VCL (curvilinear velocity, µm/s), VAP (angular path velocity, µm/s) and the movement style parameters of spermatozoa such as LIN (linearity, %, (VSL/VCL)*100), BCF (beat cross frequency, Hz), and ALH (amplitude of lateral displacement of the spermatozoa head, µm) (Özgür et. al., 2019) are examined in the study. For CASA system, it was used model of BASA-Sperm Aqua which has an Olympus

BX53 microscope (200x magnification) and a CCD camera (30 fbs) by Merk Biotechnology Ltd. Co. in Turkey. In the analyzing under the microscope, the spermatozoa in semen were activated to investigate kinematic parameters with activation solution (AS) ($CaCl_2$ 1mM; Tris 20 mM, Glycine 30 mM, NaCl 125 mM; pH 9) (Özgür et al., 2018) at ratio 1:20 (Semen:AS) under a microscope. The final dilution rate was 2000 times.

Oxidative stress indices of spermatozoa

The sperm samples were collected in a plastic tube to prepare homogenates and 500 uL PBS (50 mM, pH 7.4) was added to each tube. The homogenization process was occurred in cold media, each sample was sonified 6 cycles between each cycle 15 seconds with an ultrasonifier. Then, the homogenates were centrifuged at 10.000 rpm for 10 min at 4°C, supernatants were separated from pellets, and the pellets were stored for further analysis. In the beginning, to estimate the protein level in the supernatants, the Bradford method was take-place and bovine serum albumin (BSA) was used as a standard (Bradford 1976). After that, antioxidant enzymes were assayed. For instance, CAT activity was measured by following the decrease in the absorbance of hydrogen peroxide (H_2O_2) at 240 nm at room temperature (Aebi 1984). One unit of CAT represents the amount of enzyme that hydrolysis 1 μmol of H_2O_2 per minute. SOD activity was measured by using the xanthine oxidase/cytochrome C method reported by McCord and Fridovich (McCord and Fridovich 1969). One unit of SOD activity is the amount of the enzyme required to cause a half-maximal inhibition of cytochrome C reduction. Besides, tGSH was obtained spectrophotometrically by using the reported previous method (Akerboom and Sies 1981). The colorimetric assay was followed the increase in the formation of 5-thio-2-nitrobenzoate (TNB) which is measured spectrophotometrically at 412 nm. Malondialdehyde (MDA) is a biomarker for lipid peroxidation. The MDA level of samples was assayed via the method described by Buege and Aust (Buege and Aust 1978). CAT and SOD levels were expressed as U/mg protein, while the MDA and tGSH results were presented as nmol/mg protein.

The analysis of DNA fragmentation in spermatozoa using Comet assay

The comet assay was performed under alkaline condition. During the experiment, a version adapted to spermatozoa in study of Singh et al. (1988) was utilized (Singh et al. 1988). Previously chilled microscope slides were dipped into 0.7% extremely hot (approximately 70°C) normal melting agarose prepared in phosphate buffered saline (PBS) solution. Afterwards, 10 μL (~ 100,000 cells) of previously diluted spermatozoa was mixed with 90 μL low melting point agarose (LMA, prepared as 0.5% in PBS) and then, 70 μL of the mixture was added onto the prepared normal melting agarose covered microscope slides as a bottom layer. The slides including negative control (just spermatozoa) and positive control (spermatozoa treated with 35% of hydrogen peroxide) were put on a frozen flat tray for 10 minutes to solidify. Before using ice-cold lysis solution (2.5 M NaCl, 100 mM EDTA, 10 mM Tris base, pH 10), 1% Triton X-100 and 10% DMSO were added into the solution. Prepared slides were then cautiously immersed in lysis solution for at least 1 hour at 4°C. Slides were then removed from the lysis buffer and

placed in an electrophoresis tank. The electrophoresis tank was filled with freshly prepared electrophoresis buffer (0.3 M NaOH, 1 mM EDTA, pH 13). Before electrophoresis, the slides were left in the electrophoresis solution for 30 minutes to allow unwinding of DNA. After this procedure, electrophoresis system was turned on for 30 min at 300 mA and 15 V. After electrophoresis, slides were taken from the horizontal tank and washed three times with 0.4 M Tris buffer, pH 7.5 for 5 minutes to neutralize the alkali condition. For each slide, 60 µL of ethidium bromide (EtBr concentration: 20 mg/mL) was pipetted into the sample. Then, slides were covered with a coverslip and taken images using the inverted microscope (*Olympus CKX41*) with a combined fluorescence system at 40X magnification with *Olympus cellSens Entry 2.1* software. Comets are formed upon the principle of releasing damaged DNA from the core of the nucleus during electrophoresis. In terms of tail length, tail & head intensities, tail & head DNA percentages, 100 cells per sample (two duplicate sample slides, 50 randomly selected cells scored per slide) were scored using image analysis software *CometScore 2.0*. Totally, 100 cells were scored per slide in duplicate. Analysis was performed blindly by one slide reader. DNA fragmentation/damage scoring is classified based on the size of the comet tail: class 0, undamaged (intact) DNA; 1, 2, 3, and 4 classes of damages meaning from the less to the most fragmented cells.

Statistics analysis

Normality test and descriptive analysis (Means ± SE, $p < 0.05$) were performed between the data in the SPSS 15 program. The differences between groups were done by Variance Analysis (one-way ANOVA) with the Tukey test after the Test of Homogeneity of Variance in each group. Graph Pad Prism 5 for drawing graphics was used.

For DNA damages/fragmentation analysis in spermatozoa using Comet assay, the compliance of data to normal distribution was examined with Kolmogorov-Smirnov test. The data were summarized with median, minimum, and maximum values. Since all groups did not conform to normal distribution, Kruskal-Wallis test and then Conover pairwise comparison method was used for comparisons. The significance level was accepted as 0.05 and 0.001 tails and head of spermatozoa. Moreover, a biostatistics web application was also used for the boxplot graphs (Arslan et. al., 2018).

Results

Characterization of Cr_2O_3-Ps

The Cr_2O_3-Ps used in the study were primarily characterized by using FTIR and X-ray spectrum. Basic morphological features and basic Cr_2O_3 surface analysis were examined by SEM analysis. Its structural purity and elemental map were measured by EDX analysis. Thermal properties of the synthesized Cr_2O_3-Ps were determined by TGA and DTA thermograms.

FTIR spectrum of Cr_2O_3-Ps is given in Fig. 1. Three main regions in the FTIR spectrum of Cr_2O_3-Ps are clearly seen. The first region between 400–800 cm^{-1}, the second region between 2000–2800 cm^{-1}, and

the last region between 2800 cm^{-1} and 3700 cm^{-1} are seen. First of all, Cr-O stress vibrations are seen at 560 cm^{-1} and 650 cm^{-1}. Especially a strong metal-oxygen stretching vibration at 650 cm^{-1} proves the synthesized Cr_2O_3-Ps. In addition, an H bond peak between 2900–3600 cm^{-1} is observed stem from absorbed moisture. This peak is due to the OH groups on the Cr_2O_3 surface. In addition, a small peak is seen around 428 cm^{-1} due to absorbed moisture in the structure (Sone et al. 2016).

The X-ray spectrum of the synthesized Cr_2O_3-Ps was showed Fig. 1. In this spectrum, there are peaks confirming the Cr_2O_3-Ps, especially in the 20–70 2-theta (2θ) range. (012), (104), (110), (113), (202), (024), (116), (122), (214) and (300) peaks are visible. These peaks prove the desired Cr_2O_3-Ps when compared with the literature (Abdullah et al. 2014).

SEM images of the obtained Cr_2O_3-Ps are given in Fig. 2 at different magnifications. It is seen in these images that the Cr_2O_3-Ps structure obtained is quite pure, homogeneous, and clean. No residual starting material and foreign phase are visible. It has been proven that the desired pure and homogeneous Cr_2O_3-Ps was obtained.

The hydrodynamic diameter measurements (± standard error) for the Cr_2O_3 structures used in this study are shown in Fig. 4. According to this Figure, DLS size distribution for the Cr_2O_3-Ps is about 222 ± 125 nm and this distribution has been observed in a very narrow range (Fig. 3).

The EDX spectrum of the Cr_2O_3-Ps obtained is given in Fig. 3. On this spectrum, only peaks belonging to Cr and O are clearly seen. It is seen that the peaks of Cr in the structure are at 0.52, 5.48, and 5.91 keV values and are in harmony with the literature (Abdullah et al. 2014). The peak belonging to O is seen as a clear and clear Kα peak at 0.54 keV. Other peaks on the spectrum are Au and Pd peaks during surface coating.

Thermal properties, another basic feature of Cr_2O_3-Ps, are given in Fig. 3 with DTA and TGA thermograms. When these curves are examined in general, a mass loss of only 1.9% is observed due to the degradation of the starting material. This result proves that the Cr_2O_3 synthesis takes place with approximately 98.1% yield. In DTA thermograms of Cr_2O_3-Ps, there is no thermal change between 30°C and 1000°C. This situation confirms the purity of the metal oxide. These results prove that the desired homogeneous and pure Cr_2O_3-Ps were obtained.

The cytotoxicity of Cr_2O_3-Ps on biochemical parameters and the functions of spermatozoa

The cytotoxic effects of Cr_2O_3-Ps were observed on functions such as the velocities of spermatozoa. The spermatozoa velocities which are the VSL, VCL, and VAP values significant ($p < 0.05$) decreased after 100 µ/L dose of Cr_2O_3-Ps with compared control group. Besides, the lowest values of these velocities were

observed at the dose of 1000 µg/L. however, after Cr_2O_3-Ps exposure, it was determined that there was no significant difference ($p > 0.05$) between 500 and 1000 µg/L in the velocities of spermatozoa.

According to our results, the cytotoxic effects as the functional deformations of spermatozoa were also investigated on the movement style of spermatozoa. For example, although the value of LIN decreased in dependent on 100 µ/L dose of Cr_2O_3-Ps, it increased at 500 or 1000 doses of Cr_2O_3-Ps. While there was significant ($p < 0.05$) difference between these doses, it was not determined statistically difference ($p > 0.05$) with compared control group. The value of ALH showed decreased with increasing doses of Cr_2O_3-Ps and its decreasing was significant ($p < 0.05$) difference after 100 µ/L dose with compare control group. The value of BCF and MAD values were statistically insignificant ($p > 0.05$) with up to Cr_2O_3-Ps doses according to control groups (Table 1, Fig. 4).

Table 1
The kinematic parameters of rainbow trout spermatozoa after exposed Cr_2O_3-Ps

Parameters	N = 6	Mean ± S.E.	95% Confidence Interval for Mean	
			Lower Bound	**Upper Bound**
VSL (μm/s)	**Control**	31.45 ± 1.17^{c}	28.446	34.458
	10 μg/L	28.73 ± 0.61^{c}	27.170	30.292
	50 μg/L	28.75 ± 0.69^{c}	26.991	30.515
	100 μg/L	16.57 ± 0.44^{b}	15.439	17.705
	500 μg/L	15.14 ± 0.81^{ab}	13.051	17.231
	1000 μg/L	12.02 ± 0.52^{ab}	10.697	13.343
VCL (μm/s)	**Control**	120.86 ± 4.11^{c}	110.299	131.428
	10 μg/L	106.41 ± 2.62^{c}	99.683	113.142
	50 μg/L	105.65 ± 2.26^{c}	99.849	111.449
	100 μg/L	71.28 ± 6.32^{b}	55.028	87.529
	500 μg/L	50.90 ± 2.05^{a}	45.634	56.160
	1000 μg/L	38.67 ± 2.22^{a}	32.967	44.381
VAP (μm/s)	**Control**	54.12 ± 7.02^{c}	36.067	72.168
	10 μg/L	48.56 ± 4.75b^{c}	36.343	60.778
	50 μg/L	46.23 ± 5.20b^{c}	32.878	59.585
	100 μg/L	32.10 ± 2.62^{ab}	25.355	38.838
	500 μg/L	30.74 ± 3.05^{ab}	22.896	38.581
	1000 μg/L	19.50 ± 1.73^{a}	15.047	23.948
LIN (%)	**Control**	26.06 ± 0.69^{ab}	24.290	27.826
	10 μg/L	24.86 ± 1.66^{ab}	20.591	29.128
	50 μg/L	26.02 ± 1.87^{ab}	21.206	30.839

Data are presented Mean ± SE of values. Different letters as ^{a,b,c} show differences between groups ($p < 0.05$).

	100 µg/L	21.11 ± 2.06[a]	15.819	26.402
	500 µg/L	29.97 ± 1.93[b]	25.006	34.942
	1000 µg/L	31.48 ± 1.85[b]	26.733	36.217
BCF (Hz)	**Control**	5.46 ± 0.75	3.545	7.377
	10 µg/L	8.61 ± 1.43	4.938	12.279
	50 µg/L	5.04 ± 1.20	1.952	8.135
	100 µg/L	5.73 ± 1.21	2.614	8.853
	500 µg/L	6.52 ± 1.38	2.980	10.050
	1000 µg/L	5.63 ± 0.81	3.561	7.699
ALH (µm)	**Control**	30.31 ± 3.85[b]	20.417	40.198
	10 µg/L	21.61 ± 1.51[ab]	17.730	25.485
	50 µg/L	22.42 ± 1.75[ab]	17.915	26.923
	100 µg/L	19.45 ± 1.67[a]	15.172	23.730
	500 µg/L	17.93 ± 1.16[a]	14.953	20.902
	1000 µg/L	16.07 ± 1.24[a]	12.876	19.270
MAD (^{0})	**Control**	0.04 ± 0.006	0.021	0.054
	10 µg/L	0.03 ± 0.004	0.018	0.040
	50 µg/L	0.04 ± 0.008	0.018	0.060
	100 µg/L	0.03 ± 0.004	0.023	0.043
	500 µg/L	0.03 ± 0.004	0.020	0.041
	1000 µg/L	0.04 ± 0.005	0.022	0.048

Data are presented Mean ± SE of values. Different letters as [a,b,c] show differences between groups ($p < 0.05$).

According to our results, there was significant ($p < 0.05$) decrease in the levels of CAT and SOD with increasing concentrations of Cr_2O_3-Ps. However, the CAT activity decreased after 500 µg/L dose of Cr_2O_3-Ps, while the levels of SOD activity decreased after 100 µg/L dose of Cr_2O_3-Ps compare control group. Meanwhile, although the dose of 100 mg/L Cr_2O_3-Ps significantly increased the MDA level compared to the control group ($p < 0.05$), it was observed insignificant ($p > 0.05$) difference at tGSH levels according to all groups (Table 2, Fig. 4).

Table 2
Biochemical stress indices of rainbow trout spermatozoa after exposed Cr_2O_3-Ps

Parameters	N = 6	Mean ± S.E.	95% Confidence Interval for Mean	
			Lower Bound	**Upper Bound**
CAT (U/mg protein)	**Control**	20.44 ± 1.63^{b}	16.248	24.634
	10 µg/L	20.17 ± 1.74^{b}	15.703	24.634
	50 µg/L	18.26 ± 0.97^{ab}	15.765	20.746
	100 µg/L	17.94 ± 1.14^{ab}	15.009	20.865
	500 µg/L	13.48 ± 1.57^{a}	9.441	17.519
	1000 µg/L	12.51 ± 1.13^{a}	9.606	15.422
SOD (U/mg protein)	**Control**	6.99 ± 0.62^{b}	5.393	8.583
	10 µg/L	5.52 ± 0.18^{ab}	5.051	5.985
	50 µg/L	5.81 ± 0.33^{ab}	4.957	6.654
	100 µg/L	4.76 ± 0.25^{a}	4.110	5.407
	500 µg/L	4.43 ± 0.33^{a}	3.575	5.275
	1000 µg/L	4.30 ± 0.33^{a}	3.445	5.162
MDA (nmol/mg protein)	**Control**	1.43 ± 0.04^{a}	1.318	1.535
	10 µg/L	1.58 ± 0.10^{ab}	1.328	1.835
	50 µg/L	1.52 ± 0.04^{ab}	1.415	1.631
	100 µg/L	1.83 ± 0.11^{b}	1.554	2.102
	500 µg/L	1.60 ± 0.09^{ab}	1.375	1.828
	1000 µg/L	1.60 ± 0.12^{ab}	1.306	1.897
TGSH (nmol/mg protein)	**Control**	15.92 ± 1.14	12.994	18.846
	10 µg/L	14.68 ± 0.98	12.157	17.207
	50 µg/L	16.53 ± 1.88	11.694	21.369

Data are presented Mean ± SE of values. Different letters as ^{a,b,c} show differences between groups ($p < 0.05$).

	100 µg/L	16.40 ± 1.11	13.541	19.264
	500 µg/L	14.84 ± 1.31	11.463	18.218
	1000 µg/L	18.07 ± 1.91	13.152	22.983

Data are presented Mean ± SE of values. Different letters as [a,b,c] show differences between groups ($p < 0.05$).

Additionally, it was calculated effective doses for spermatozoa velocities against exposure of Cr_2O_3-Ps. The effective concentration (EC50) is the concentration of toxicant at which the toxicant is half of the maximum effective. In this study, the EC50 against exposure of Cr_2O_3-Ps was determined in values of VSL and VCL, 76.67 µg/L and 87.77 µg/L (Fig. 4), respectively.

The genotoxicity of Cr_2O_3-Ps on DNA of spermatozoa

The detection of DNA fragmentation/damage using Comet assay, especially in spermatozoa, is a greatly beneficial and accurate way of explaining environmental toxicology (Singh et al., 1988). Furthermore, DNA damage in spermatozoa is related not only toxic effects at that time but also affecting next generation of aquatic organisms. Thus, DNA-fragmented spermatozoa exposed to environmental pollutants occur a reduction in hatching success as well as abnormalities in embryo development (Pérez-Cerezales et al. 2010). Our research has an extremely significant impact as being the first article because of investigating the genotoxic effect of Cr_2O_3 particles on the spermatozoa of rainbow trout (*Oncorhynchus mykiss*) in the literature.

According to DNA evaluation by Comet assay on Fig. 5, the spermatozoa in the (-) control had undamaged cells; on the other hand, the spermatozoa treated with hydrogen peroxide (H_2O_2) also known as (+) control had extremely damaged cells compared to the spermatozoa with Cr_2O_3-Ps. In addition, the spermatozoa of rainbow trout (*Oncorhynchus mykiss*) exposed the different concentrations of Cr_2O_3-Ps revealed significantly higher DNA damages in when compared to the negative control. DNA fragmentation was detected in all spermatozoa after acute exposure. Using Comet assay images from Fig. 5, it is clearly seen that damages in DNA increase with gradually augmented concentrations of Cr_2O_3 particles. Thus, effects of Cr_2O_3 particles on DNA fragmentation of spermatozoa have been detected and described as dose dependent manner.

Presented features of spermatozoa may explain us tail length (pixels), which is length of the tail in pixels, boxplot showed in Fig. 6B, as Cr_2O_3 particles make rainbow trout spermatozoa (*Oncorhynchus mykiss*) lost DNA intact and have longer tail lengths with increasing particle concentrations.

Tail DNA (%) means tail DNA content as a percentage of comet DNA content whereas Head DNA (%) is head DNA content as a percentage of comet DNA content. As shown in Fig. 3, head DNA (%) values have been ranging from 86.88 ± 7.76% to 75.79 ± 10.66% conversely to tail DNA (%) depending on the specific concentration of Cr_2O_3 particles. Significantly higher DNA damages have been gradually observed with

increasing concentrations of Cr_2O_3 particles from the data of tail DNA (%). In contrast to this data, the spermatozoa exposed to Cr_2O_3 particles exhibited lower DNA damages compared to cells treated with H_2O_2, (+) Control (Fig. 7).

The spermatozoa in the negative control had undamaged cells approximately 60% according to DNA evaluation by Comet assay from Fig. 8. The spermatozoa exposed to Cr_2O_3 particles showed significantly higher DNA damages compared to the negative control. DNA damage was detected in all spermatozoa in 50 µg/L concentration of Cr_2O_3 particles. Moreover, spermatozoa in Class 0 were not observed for Cr_2O_3 particles having 1000 µg/L concentration.

Values related to Tail Intensity (Pixels), Head Intensity (Pixels), Tail DNA (%), Head DNA (%), Tail length (Pixels), and Tail Moment, which is defined as Tail length (Pixels) x Tail DNA (%) in Table 3 and Table 4.

Table 3
The comparisons between the percentages of DNA in Head (%), DNA in Tail (%), and Tail Moment using Comet Assay of rainbow trout spermatozoa. The different concentrations of Cr_2O_3 -Ps, (-) and (+) controls expressed as Median (Min – Max)

Groups	DNA in Head (%) Median (Min – Max)	DNA in Tail (%) Median (Min – Max)	Tail Moment Median (Min – Max)
(-) Control[a]	82.99 (70.99–93.4)[bcfg]	17.01 (6.6–29.01)[bcfg]	0.3 (0.07–2.03)[bg]
(+) Control (H_2O_2)[b]	79.57 (7.69–97.22)[acde]	20.43 (0.28–92.31)[acde]	0.55 (0.06–23.68)[acdf]
10 µg/L[c]	88.79 (67.44–99.52)[abefg]	11.21 (0.48–32.56)[abefg]	0.23 (0–2.3)[befg]
50 µg/L[d]	85.57 (67.53–97.29)[bfg]	14.43 (2.71–32.47)[bfg]	0.22 (0.03–2.98)[befg]
100 µg/L[e]	83.71 (54.85–94.53)[bcg]	16.29 (5.47–45.15)[bcg]	0.4 (0.06–6.32)[cdg]
500 µg/L[f]	79.18 (57.79–91.63)[acd]	20.82 (8.37–42.21)[acd]	0.38 (0.09–8.02)[bcdg]
1000 µg/L[g]	78.73 (37.82–87.13)[acde]	21.27 (12.87–62.18)[acde]	0.6 (0.14–6.84)[acdef]
p	< 0.001	< 0.001	< 0.001
Min, minimum; Max, maximum.			
[a]: significant from the negative control (a); [b]: significant from the positive control (b); [c]: significant from (c); [d]: significant from (d); [e]: significant from (e); [f]: significant from (f); [g]: significant from (g). The values (n = 100) are Median (Min – Max) with common superscripts in the same line are significantly different.			

Table 4
The dose-dependent effects of Cr_2O_3-Ps on genotoxicity parameters of rainbow trout spermatozoa after acute exposure

Parameters	Head Intensity (Pixels)	DNA in Head (%)	Tail Intensity (Pixels)	Tail Length (Pixels)	DNA in Tail (%)	Tail Moment
(-) Control[a]	47183.44 ± 10921.84[bcfg]	83.72 ± 5.3[bcfg]	8814.06 ± 2519.2	2.34 ± 1.51[bg]	16.28 ± 5.3[bcfg]	0.42 ± 0.39[bg]
(+) Control (H_2O_2)[b]	28358.78 ± 18114.05[acdefg]	70.73 ± 21.89[acde]	11170.98 ± 14060.22[cg]	6.94 ± 8.6[acdf]	29.27 ± 22.06[acde]	3.12 ± 5.52[acdf]
10 µg/L[c]	83807.06 ± 55963.65[abdefg]	86.88 ± 7.76[abefg]	10941.36 ± 5579.83[bd]	2.64 ± 1.95[bg]	13.12 ± 7.76[abefg]	0.37 ± 0.45[befg]
50 µg/L[d]	44825.24 ± 16163.64[bcfg]	84.71 ± 7.72[bfg]	8038.12 ± 5027.89[cg]	2.68 ± 2.24[bg]	15.29 ± 7.72[bfg]	0.49 ± 0.62[befg]
100 µg/L[e]	47042.28 ± 20393.44[bcfg]	81.76 ± 8.28[bcg]	10035.4 ± 6086.71	3.68 ± 3.35	18.24 ± 8.28[bcg]	0.83 ± 1.25[cdg]
500 µg/L[f]	38465.52 ± 18634.98[abcde]	78.59 ± 8.82[acd]	10449.36 ± 8936.16	3.48 ± 3.96[bg]	21.41 ± 8.82[acd]	0.84 ± 1.31[bcdg]
1000 µg/L[g]	36698.08 ± 14178.36[abcde]	75.79 ± 10.66[acde]	11496.38 ± 7660.65[bd]	4.04 ± 2.89[acdf]	24.21 ± 10.66[acde]	1.13 ± 1.24[acdef]

The values (n = 100) are mean ± standard deviation with common superscripts in the same line are significantly different.

[a]: significant from the negative control (a); [b]: significant from the positive control (b); [c]: significant from (c); [d]: significant from (d); [e]: significant from (e); [f]: significant from (f); [g]: significant from (g).

Discussion

This study investigated the cytotoxic effects of different doses (10, 50, 100, 500, and 1000 µ/L) Cr_2O_3-Ps on spermatozoa of rainbow trout (*Oncorhynchus mykiss*) *in vitro* conditions. For this target, the cytotoxic effects were analyzed the functional deformations in the velocities, movement styles, enzymatic activities, and DNA damages of spermatozoa, the end of the study was determined effective concentrations of Cr_2O_3-Ps.

In this study, Cr_2O_3-Ps caused changes in the physical and biochemical functions in spermatozoa of rainbow trout. In light of the literature for functional deformations, there are same results which are parallel with our data. For example, lower doses than 100 µg/mL dose of Cr_2O_3-Ps showed minimum toxicity on viability or apoptosis of two human lung cell lines, BEAS-2B and A549 (Chusuei et al. 2013).

Another hand, high doses such as 300 cm^2/mL of Cr_2O_3-Ps had a negative on the function and mechanism of epithelial cells, monocytic/macrophage cells, human erythrocytes, and combined culture (Cho et al. 2013). However, it was observed morphological damages and partially disintegration in body of *Daphnia similis* (Tavares et al. 2014). However, especially the functional negative effects were shown on the enzyme activities and DNA fragmentations of spermatozoa with dose-dependent manner of Cr_2O_3-Ps in our study. Similarly, it was determined the negative effects such as significant growth inhibitory and cell membrane damage and oxidative stress responses in ROS on *Escherichia coli* after exposure of Cr_2O_3-Ps (Kaweeteerawat et al. 2015). The exposure to Cr_2O_3-Ps on green alga showed cytotoxic effects such as inhabitation growth, lowered chlorophyll content, increasing ROS levels (Costa et al. 2015). Other hand, it was found the negative biological functions such as longevity, reproduction, and growth parameters of *Daphnia magna after* Cr_2O_3-Ps exposure (Puerari et al. 2016) and the diversity of bacterial communities and inhibited the enzyme activity analysis (Wang et al. 2017).

Nano or micro particles have also harmful effects on the functional structures of cells such as reduced cell viability and inhibited proliferation (Agrawal and Kango 2019), reduction of spermatozoa velocities (Özgür et al. 2018a) with DNA damage and enzyme activities (Préaubert et al. 2018; Agrawal and Kango 2019; Barkhade et al. 2019; Nikolovski et al. 2019; Santonastaso et al. 2019). In our results, the velocities (VSL, VCL, and VAP) and the movement styles (ALH and LIN) of spermatozoa were negative affected by dose-dependent manner of Cr_2O_3-Ps, and these results were parallel with data of above literatures.

The cytotoxic effects of Cr_2O_3-Ps were observed changes in enzymatic activities in spermatozoa. Biochemical parameters of spermatozoa such as CAT, SOD, MDA and tGSH as oxidative stress indices were measured after Cr_2O_3-Ps exposure. SOD catalyzes the conversion of superoxide (O_2^-) radical to H_2O_2, while CAT carries out the conversion of H_2O_2 to water and oxygen. Therefore, the SOD-CAT system provides the first defense against oxygen toxicity (Afifi et al. 2016). According to our results, there was a significant decrease in the levels of CAT and SOD with increasing concentrations of Cr_2O_3-Ps. This decrease in both SOD and CAT levels may have been caused by the excessive ROS production induced by Cr_2O_3-Ps. The same results were reported by Afifi et al. (Afifi et al. 2016). They investigated the toxicity effect of Ag-NPs on *Oreochromis niloticus* and *Tilapia zillii.* While 2 mg/L Ag-NPs did not lead to any significant change in the SOD and CAT levels, dose of 4 mg/L showed a significant reduction in the levels. Similarly, our previous study reported that SOD and CAT levels were significantly decreased after exposure to 100 mg/L of Fe_3O_4 NPs (Özgür et al. 2018b). In our study, While MDA level significantly increased compared control group, tGSH levels did not change. MDA is an important biomarker to determine lipid peroxidation. This increase in MDA level after exposure to the Cr_2O_3-Ps could be due to the depletion of the antioxidant system, which is consistent with the aforementioned results. Also, Cr ions produced from Cr_2O_3-Ps are incriminated from increased lipid peroxidation (Sinha et al. 2005). Additionally, our outcomes were enforced by the results of Adebayo et al. (Adebayo et al. 2018). Other hand, it is well known that GSH protects the biological systems from oxidative stress. Mechanisms of change in the tGSH level may be different. For instance, excessive ROS production may have affected

tGSH levels. Alternatively, the Cr ions may have shown inhibition on GSH-synthesizing enzymes. Maybe both are involved.

Investigating the effects of UV radiation and hydrogen peroxide (used as oxidative agents) on rainbow trout, *Oncorhynchus mykiss*, spermatozoa, Dietrich et al. (2005) found a decrease in sperm motility and DNA integration after a long duration of UV. From our research, H_2O_2 effect on a spermatozoa cell has been observed as (+) Control from Fig. 2A. Dose-dependent reductions in sperm motility and fertilizing features were significantly changed after spermatozoa were exposure to H_2O_2. Exposed of rainbow trout spermatozoa to some elements such as mercury and cadmium occurs an increase in DNA damage measured via Comet assay with brutal results in terms of sperm motility and hatching rate (Dietrich et al. 2005). Unlike oocytes, fish spermatozoa have been known not to have efficient evolutional defense mechanisms like DNA repairing against environmental pollutants even though having extremely condensed genetic material, DNA (Aitken et al. 2004). Furthermore, after exposure to physical/chemical stresses, spermatozoa have exhibited extreme sensitivity to oxidative stress, which is responsible for DNA fragmentation, because of not having enough antioxidant defense mechanism and extreme content in unsaturated fatty acids (Labbe et al. 1995; Cabrita et al. 2010; Li et al. 2010a, b; Linhartova et al. 2013).

Conclusion

According to literatures, it is clear that chromium and its components are highly toxic for living organisms in the introduction section. However, it has known that the cytotoxicity results can be very variable because there are many reasons such as cell type, the physiological functions of cell and physical structures of particles. This study clarified the lack of information on the effects of Cr_2O_3-Ps on the reproductive functions of fish, especially sperm quality.

Finally, we concluded with all these results that may be useful data to determine the safety of Cr_2O_3-Ps in aquatic environment and ecotoxicology.

Declarations

Author contributions

Mustafa Erkan Özgür: Supervision, Review, Investigation, Methodology, Conceptualization, Formal analysis, Writing, Review & Editing. Ahmet Ulu: Investigation, Methodology, Formal analysis, Writing & editing. Canbolat Gürses: Investigation, Methodology, Formal analysis, Review & Editing. İmren Özcan: Formal analysis. Samir Abbas Ali Noma: Formal analysis. Süleyman Köytepe: Supervision, Methodology, Validation, Writing, Review & Editing. Burhan Ateş: Supervision, Review & Editing, Conceptualization.

Acknowledgment

No funding from a project but analyzes for study were supported by physicochemical and biochemical laboratories in Inönü University and Malatya Turgut Özal University. Therefore, the authors are grateful to the universities for providing the resources to develop this study.

Data availability

The datasets used and/or analyzed during the current research are available from the corresponding author on reasonable request.

Ethical approval

Not applicable.

Consent to participate

Not applicable.

Consent to publish

Not applicable.

Competing interests

The authors declare no competing interests.

References

1. Abdullah MM, Rajab FM, Al-Abbas SM (2014) Structural and optical characterization of Cr2O3 nanostructures: Evaluation of its dielectric properties. AIP Adv 4:. doi: 10.1063/1.4867012
2. Adebayo OA, Akinloye O, Adaramoye OA (2018) Cerium oxide nanoparticle elicits oxidative stress, endocrine imbalance and lowers sperm characteristics in testes of balb/c mice. Andrologia 50:e12920. doi: 10.1111/and.12920
3. Aebi H (1984) Catalase *in vitro*. In: Methods in Enzymology. pp 121–126
4. Afifi M, Saddick S, Abu Zinada OA (2016) Toxicity of silver nanoparticles on the brain of Oreochromis niloticus and Tilapia zillii. Saudi J Biol Sci 23:754–760. doi: 10.1016/j.sjbs.2016.06.008
5. Agrawal S, Kango N (2019) Development and catalytic characterization of L-asparaginase nano-bioconjugates. Int J Biol Macromol 135:1142–1150. doi: 10.1016/j.ijbiomac.2019.05.154
6. Aitken RJ, Koopman P, Lewis SEM (2004) Seeds of concern. Nature 432:48–52

7. Akerboom TPM, Sies H (1981) Assay of Glutathione, Glutathione Disulfide, and Glutathione Mixed Disulfides in Biological Samples. Methods Enzymol. doi: 10.1016/S0076-6879(81)77050-2
8. Barkhade T, Mahapatra SK, Banerjee I (2019) Study of mitochondrial swelling, membrane fluidity and ROS production induced by nano-TiO2 and prevented by Fe incorporation. Toxicol Res (Camb) 8:711–722. doi: 10.1039/c9tx00143c
9. Bradford MM (1976) A rapid and sensitive method for the quantitation of microgram quantities of protein utilizing the principle of protein-dye binding. Anal Biochem 72:248–254. doi: 10.1016/0003-2697(76)90527-3
10. Buege JA, Aust SD (1978) Microsomal Lipid Peroxidation. Methods Enzymol 52:. doi: 10.1016/S0076-6879(78)52032-6
11. Cabrita E, Sarasquete C, Martínez-Páramo S, et al (2010) Cryopreservation of fish sperm: Applications and perspectives. J. Appl. Ichthyol. 26:623–635
12. Canadian Water Quality Guidelines (1999) Canadian Water Quality Guidelines for the Protection of Aquatic Life. Can Counc Minist Environ 1–5
13. Chavali MS, Nikolova MP (2019) Metal oxide nanoparticles and their applications in nanotechnology. SN Appl Sci 1:. doi: 10.1007/s42452-019-0592-3
14. Cho WS, Duffin R, Bradley M, et al (2013) Predictive value of in vitro assays depends on the mechanism of toxicity of metal oxide nanoparticles. Part Fibre Toxicol 10:. doi: 10.1186/1743-8977-10-55
15. Chusuei CC, Wu CH, Mallavarapu S, et al (2013) Cytotoxicity in the age of nano: The role of fourth period transition metal oxide nanoparticle physicochemical properties. Chem Biol Interact 206:319–326. doi: 10.1016/j.cbi.2013.09.020
16. Costa CH da, Perreault F, Oukarroum A, et al (2015) Effect of chromium oxide (III) nanoparticles on the production of reactive oxygen species and photosystem II activity in the green alga Chlamydomonas reinhardtii. Sci Total Environ 565:951–960. doi: 10.1016/j.scitotenv.2016.01.028
17. Dietrich GJ, Szpyrka A, Wojtczak M, et al (2005) Effects of UV irradiation and hydrogen peroxide on DNA fragmentation, motility and fertilizing ability of rainbow trout (Oncorhynchus mykiss) spermatozoa. Theriogenology 64:1809–1822. doi: 10.1016/j.theriogenology.2005.04.010
18. Du J, Xu S, Zhou Q, et al (2019) The ecotoxicology of titanium dioxide nanoparticles, an important engineering nanomaterial. Toxicol. Environ. Chem. 101:165–189
19. EPA (2015) Water: Chromium In Drinking Water. In: United States Environmwntal Prot. Agency. water.epa.gov/drink/info/chromium/
20. Galwey AK, Pöppl L, Rajam S (1983) A melt mechanism for the thermal decomposition of ammonium dichromate. J Chem Soc Faraday Trans 1 Phys Chem Condens Phases 79:2143–2151. doi: 10.1039/F19837902143
21. He X, Aker WG, Fu PP, Hwang HM (2015) Toxicity of engineered metal oxide nanomaterials mediated by nano-bio-eco-interactions: A review and perspective. Environ. Sci. Nano 2:564–582

22. Kaweeteerawat C, Ivask A, Liu R, et al (2015) Toxicity of metal oxide nanoparticles in Escherichia coli correlates with conduction band and hydration energies. Environ Sci Technol 49:1105–1112. doi: 10.1021/es504259s
23. Labbe C, Maisse G, Müller K, et al (1995) Thermal acclimation and dietary lipids alter the composition, but not fluidity, of trout sperm plasma membrane. Lipids 30:23–33. doi: 10.1007/BF02537038
24. Lebedev S, Gavrish I, Rusakova E, et al (2018) Influence of various chromium compounds on physiological, morpho-biochemical parameters, and digestive enzymes activity in Wistar rats. Trace Elem Electrolytes 35:242–245. doi: 10.5414/tex0155419
25. Li J, Song Y, Wu K, et al (2018) Effects of Cr2O3 nanoparticles on the chlorophyll fluorescence and chloroplast ultrastructure of soybean (Glycine max). Environ Sci Pollut Res 25:19446–19457. doi: 10.1007/s11356-018-2132-x
26. Li P, Li ZH, Dzyuba B, et al (2010a) Evaluating the impacts of osmotic and oxidative stress on common carp (Cyprinus carpio, L.) sperm caused by cryopreservation techniques. Biol Reprod 83:852–858. doi: 10.1095/biolreprod.110.085852
27. Li ZH, Li P, Dzyuba B, Randak T (2010b) Influence of environmental related concentrations of heavy metals on motility parameters and antioxidant responses in sturgeon sperm. Chem Biol Interact 188:473–477. doi: 10.1016/j.cbi.2010.09.005
28. Linhartova P, Gazo I, Shaliutina A, Hulak M (2013) The in vitro effect of duroquinone on functional competence, genomic integrity, and oxidative stress indices of sterlet (Acipenser ruthenus) spermatozoa. Toxicol Vitr 27:1612–1619. doi: 10.1016/j.tiv.2013.04.002
29. Mahieu B, Apers DJ, Capron PC (1971) Thermal decomposition of ammonium dichromate. J Inorg Nucl Chem 33:2857–2866. doi: 10.1016/0022-1902(71)80047-7
30. Maitlo HA, Kim KH, Kumar V, et al (2019) Nanomaterials-based treatment options for chromium in aqueous environments. Environ. Int. 130
31. McCord JM, Fridovich I (1969) Superoxide dismutase. An enzymic function for erythrocuprein (hemocuprein). J Biol Chem 244:6049–6055. doi: 10.1016/0003-2697(69)90079-7
32. Nikolovski D, Cumic J, Pantic I (2019) Application of gray level co-occurrence matrix algorithm for detection of discrete structural changes in cell nuclei after exposure to iron oxide nanoparticles and 6-hydroxydopamine. Microsc Microanal 25:982–988. doi: 10.1017/S1431927619014594
33. Özgür, Mustafa Erkan; Okumuş F. K (2019) A Novel Computer Assisted Sperm Analyzer for Assessment of Spermatozoa Motility in Fish; BASA-Sperm Aqua. El-Cezeri Fen ve Mühendislik Derg. doi: 10.31202/ecjse.486342
34. Özgür ME, Balcıoğlu S, Ulu A, et al (2018a) The in vitro toxicity analysis of titanium dioxide (TiO2) nanoparticles on kinematics and biochemical quality of rainbow trout sperm cells. Environ Toxicol Pharmacol 62:11–19. doi: 10.1016/j.etap.2018.06.002
35. Özgür ME, Ulu A, Balcioğlu S, et al (2018b) The toxicity assessment of iron oxide (Fe 3 O 4) nanoparticles on physical and biochemical quality of rainbow trout spermatozoon. Toxics 6:62. doi:

10.3390/toxics6040062

36. Özgür ME, Ulu A, Özcan İ, et al (2019) Investigation of toxic effects of amorphous SiO2 nanoparticles on motility and oxidative stress markers in rainbow trout sperm cells. Environ Sci Pollut Res 26:15641–15652. doi: 10.1007/s11356-019-04941-5
37. Pérez-Cerezales S, Martínez-Páramo S, Beirão J, Herráez MP (2010) Fertilization capacity with rainbow trout DNA-damaged sperm and embryo developmental success. Reproduction 139:989–997. doi: 10.1530/REP-10-0037
38. Préaubert L, Tassistro V, Auffan M, et al (2018) Very low concentration of cerium dioxide nanoparticles induce DNA damage, but no loss of vitality, in human spermatozoa. Toxicol Vitr 50:236–241. doi: 10.1016/j.tiv.2018.03.013
39. Puerari RC, da Costa CH, Vicentini DS, et al (2016) Synthesis, characterization and toxicological evaluation of Cr2O3 nanoparticles using Daphnia magna and Aliivibrio fischeri. Ecotoxicol Environ Saf 128:36–43. doi: 10.1016/j.ecoenv.2016.02.011
40. Santonastaso M, Mottola F, Colacurci N, et al (2019) In vitro genotoxic effects of titanium dioxide nanoparticles (n-TiO2) in human sperm cells. Mol Reprod Dev 86:1369–1377. doi: 10.1002/mrd.23134
41. Singh NP, McCoy MT, Tice RR, Schneider EL (1988) A simple technique for quantitation of low levels of DNA damage in individual cells. Exp Cell Res 175:184–191. doi: 10.1016/0014-4827(88)90265-0
42. Sinha S, Saxena R, Singh S (2005) Chromium induced lipid peroxidation in the plants of Pistia stratiotes L.: Role of antioxidants and antioxidant enzymes. Chemosphere 58:595–604. doi: 10.1016/j.chemosphere.2004.08.071
43. Sone BT, Manikandan E, Gurib-Fakim A, Maaza M (2016) Single-phase α-Cr2O3nanoparticles' green synthesis using Callistemon viminalis' red flower extract. Green Chem Lett Rev 9:85–90. doi: 10.1080/17518253.2016.1151083
44. Tavares KP, Caloto-Oliveira Á, Vicentini DS, et al (2014) Acute toxicity of copper and chromium oxide nanoparticles to Daphnia similis. Ecotoxicol Environ Contam 9:43–50. doi: 10.5132/eec.2014.01.006
45. U.S Geological Survey (2020) Mineral Commodity Summaries 2020
46. Wang X, Zheng Q, Yuan Y, et al (2017) Bacterial community and molecular ecological network in response to Cr2O3 nanoparticles in activated sludge system. Chemosphere 188:10–17. doi: 10.1016/j.chemosphere.2017.08.072
47. Zhu Y, Liu X, Hu Y, et al (2019) Behavior, remediation effect and toxicity of nanomaterials in water environments. Environ. Res. 174:54–60

Figures

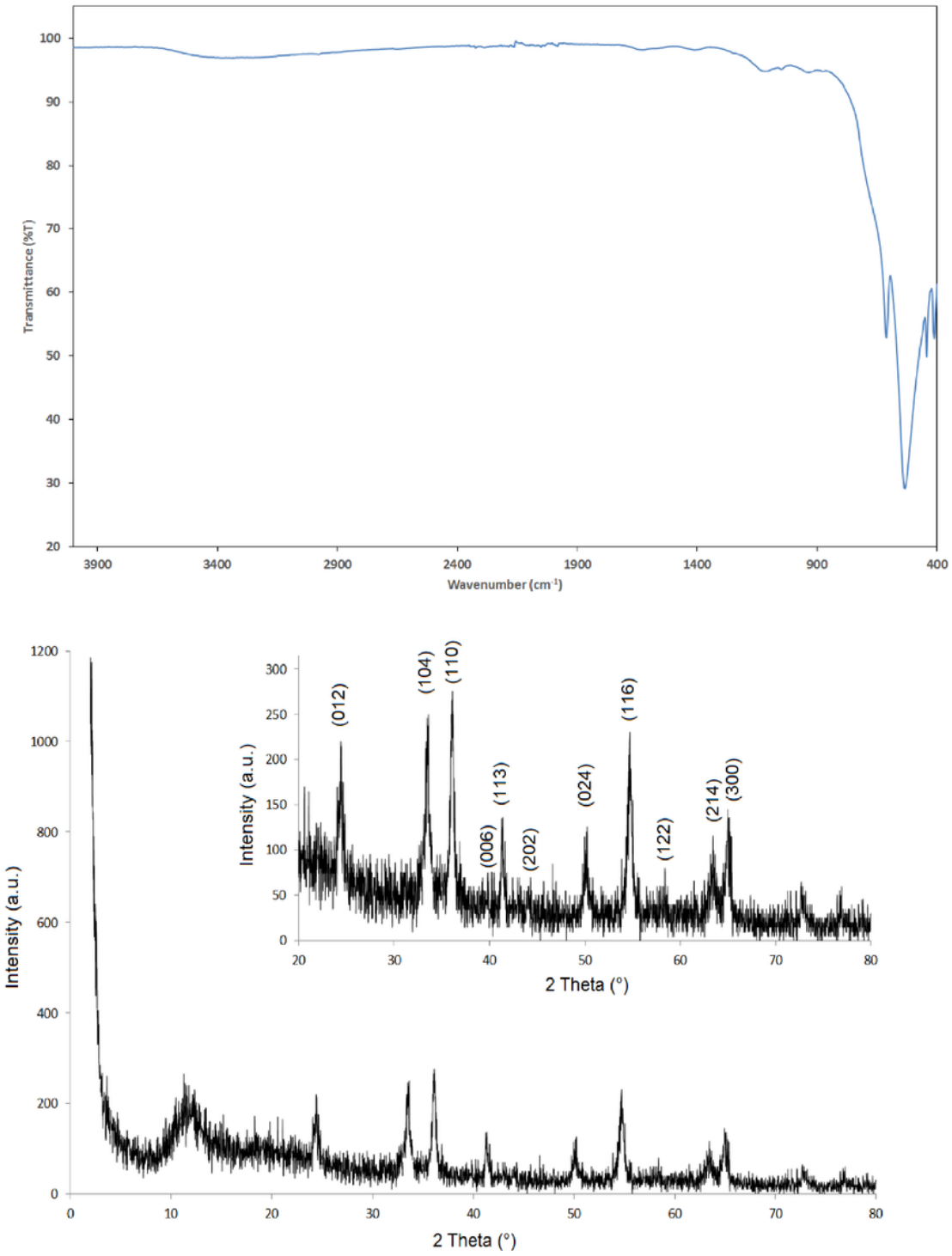

Figure 1

FTIR and X-ray spectrum of the Cr2O3 –Ps

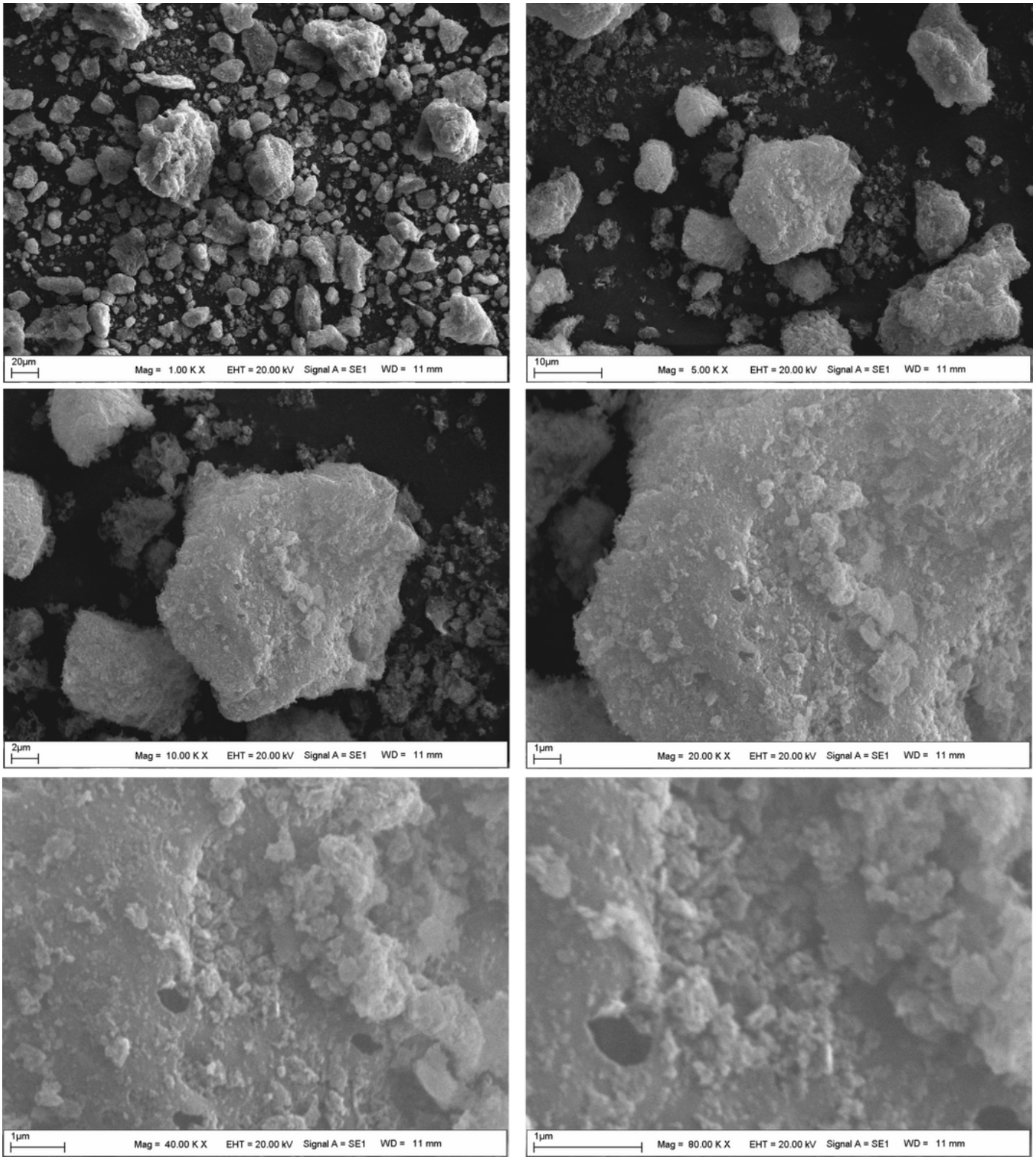

Figure 2

SEM image of the Cr2O3 -Ps with different magnifications

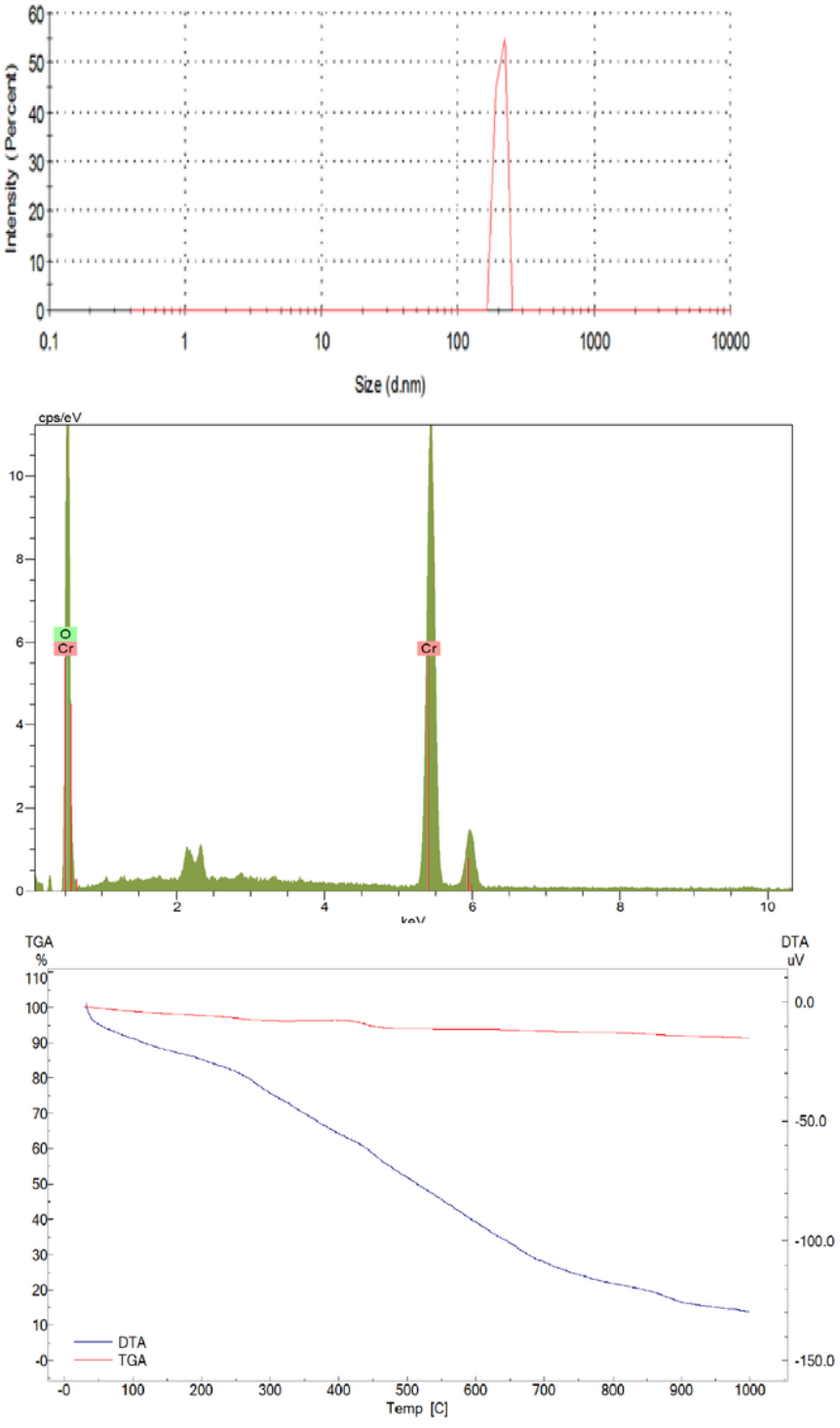

Figure 3

Hydrodynamic size distribution, EDX spectrum, TGA and DTA thermograms of Cr2O3 –Ps

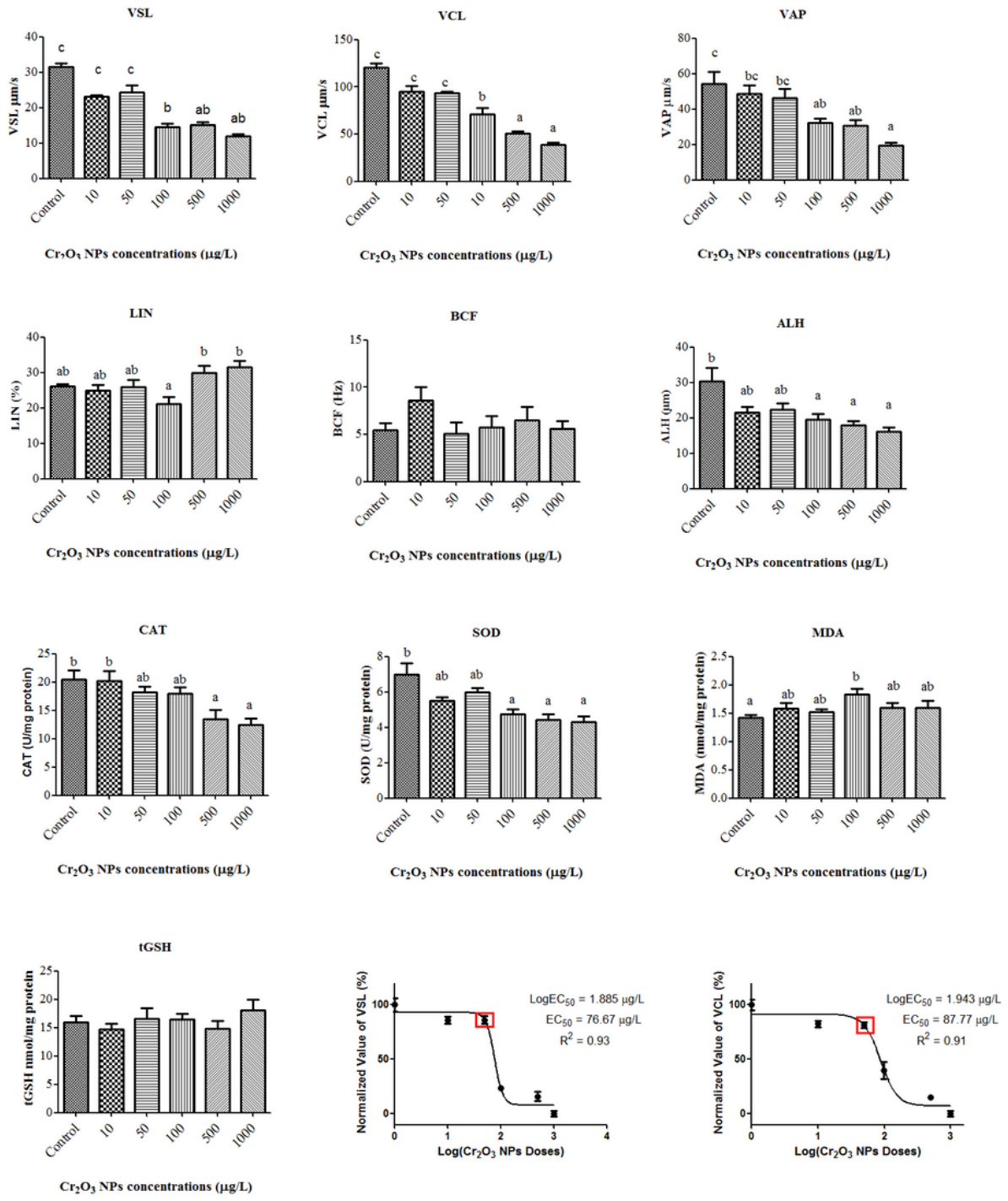

Figure 4

The kinematics, biochemical stress indices and EC50 values of spermatozoa after Cr2O3-Ps exposure

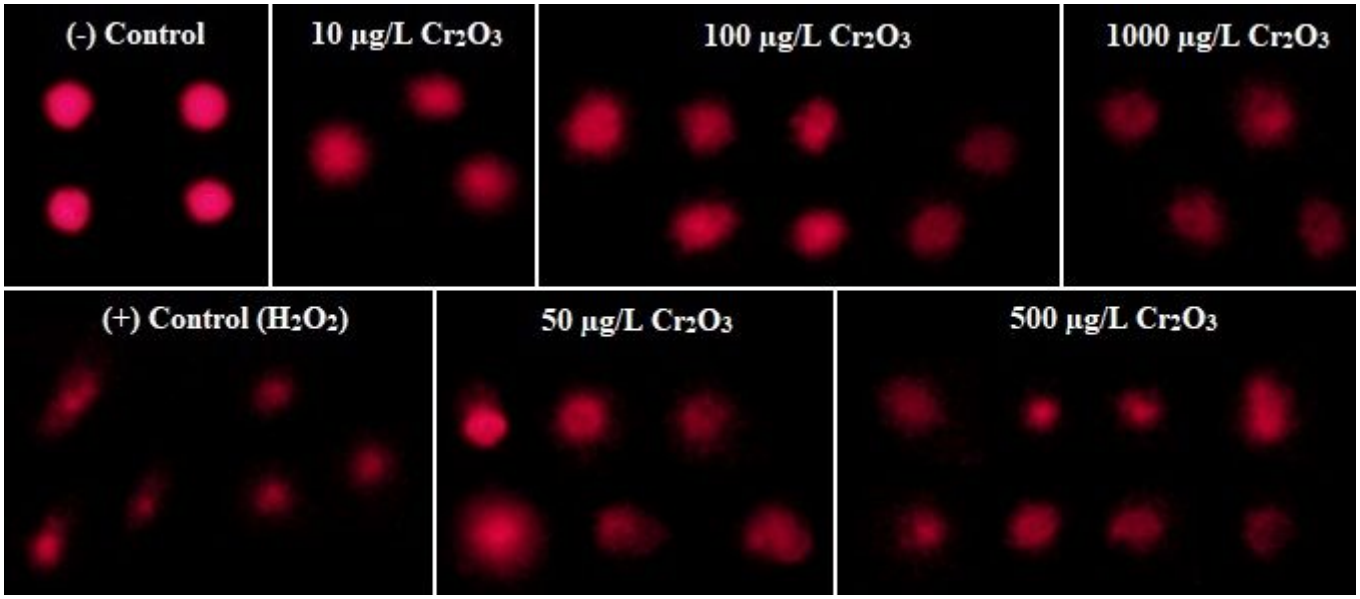

Figure 5

The different types of DNA damages in rainbow trout spermatozoa against different concentrations of Cr2O3-Ps. Each comet represents DNA fragmentations except (-) Control

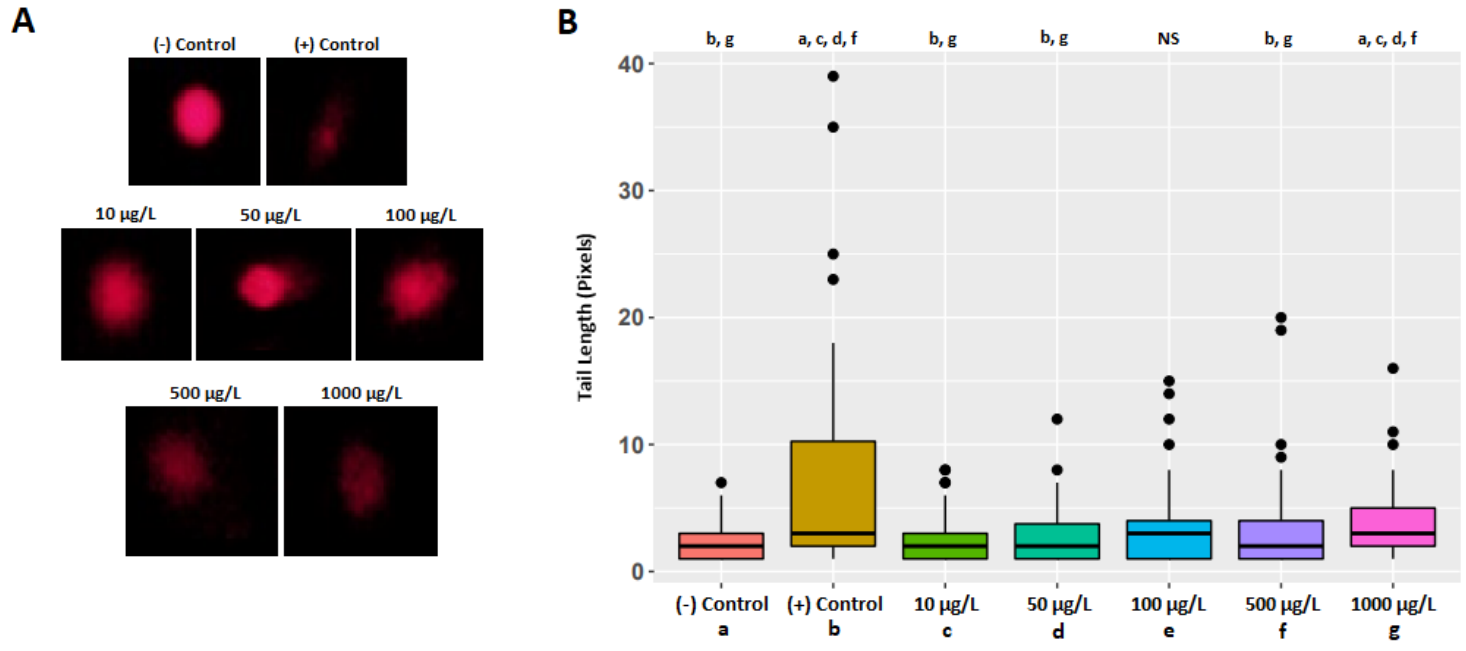

Figure 6

A) The different representative images of DNA fragmentations using Comet assay. B) The comparison of tail length (pixels) values between the negative and positive controls as well as the different concentrations of Cr2O3-Ps. The box-plot graph shows the distribution of tail length (pixels) values of spermatozoa, and the horizontal lines indicate the median values. Each experiment was done as duplicated with having 100 spermatozoa per condition analyzed. The lowercase letters above the boxplot are significantly different. a: significant from the negative control (a); b: significant from the positive

control (b); c: significant from (c); d: significant from (d); e: significant from (e); f: significant from (f); g: significant from (g). NS, not significant

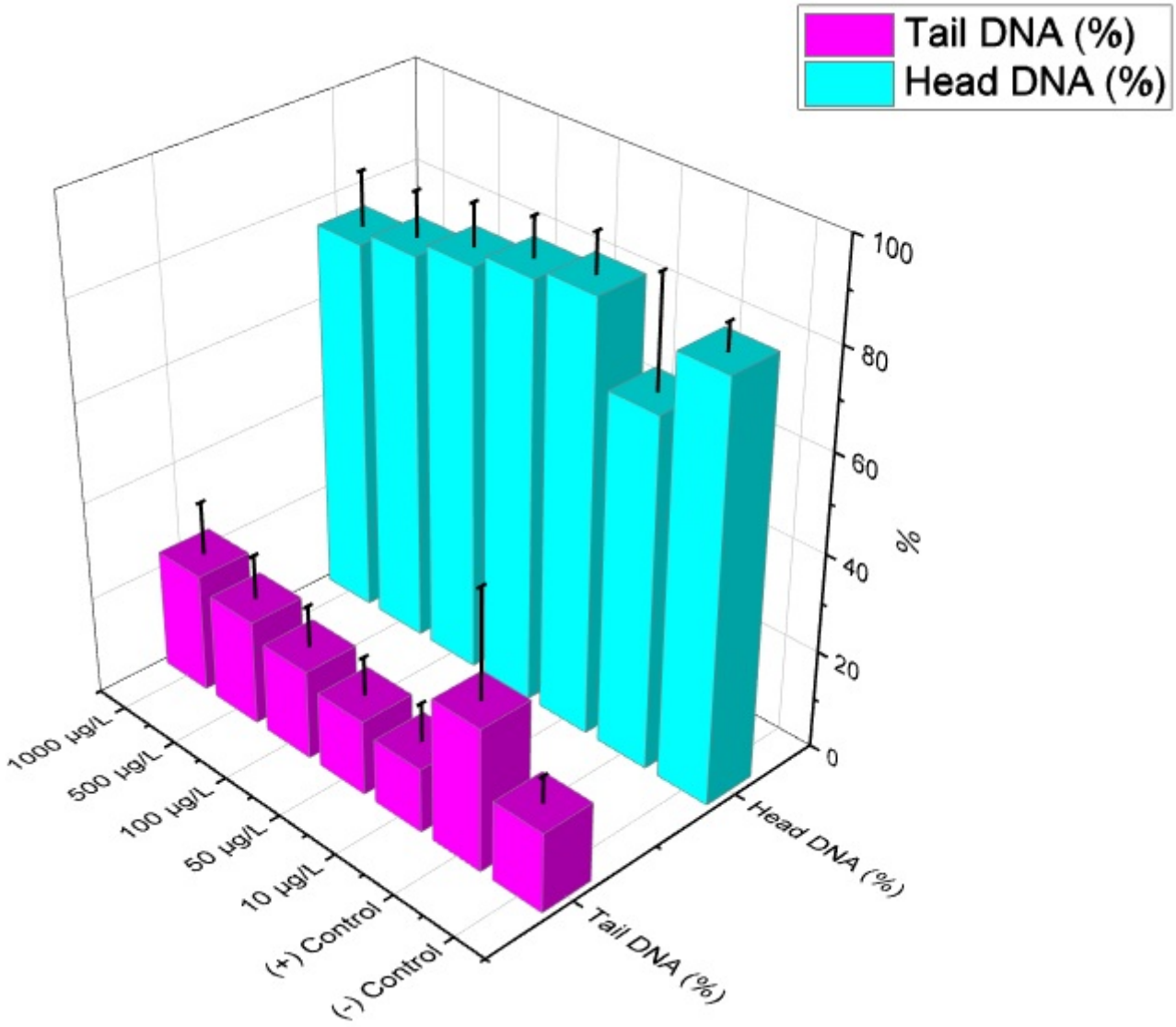

Figure 7

Genotoxicity values in terms of Tail DNA (%) and Head DNA (%) measured using Comet assay in rainbow trout spermatozoa after acute exposure of Cr2O3-Ps

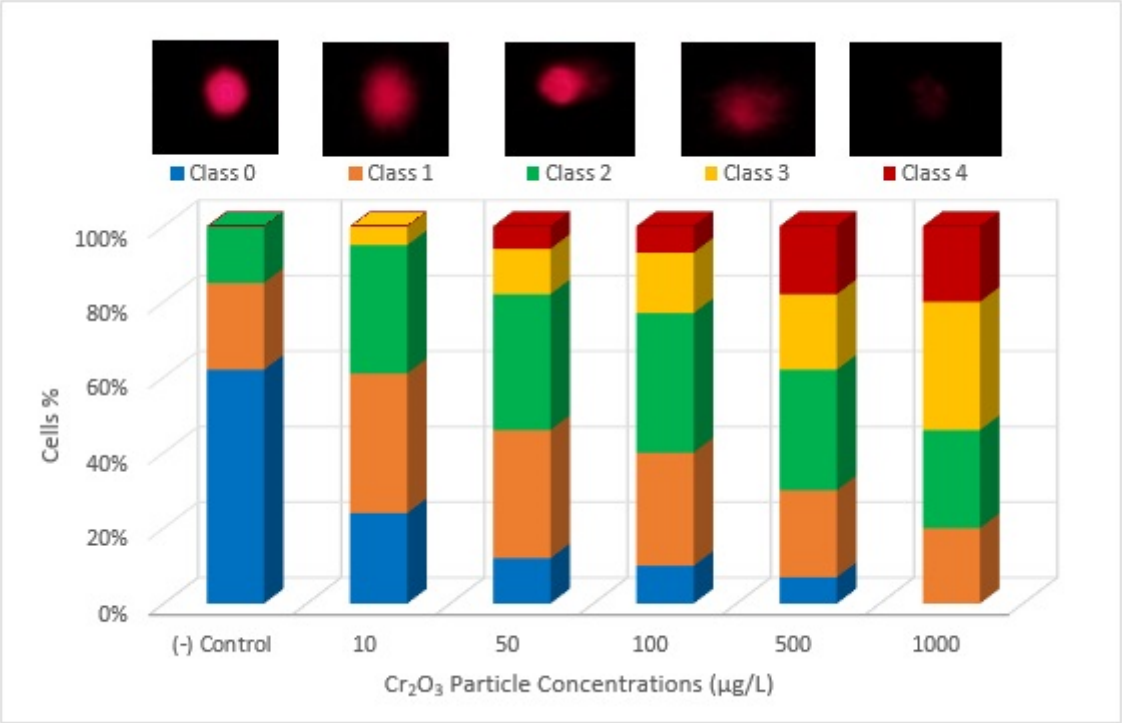

Figure 8

Effects of Cr2O3-Ps at different concentrations on DNA integrity of spermatozoa of rainbow trout

Supplementary Files

This is a list of supplementary files associated with this preprint. Click to download.

- GraphicalAbstract.png